Retrieval analysis of an explanted Mobi-C cervical disc replacement: A case study

Göksu Kandemir[a], Marina Pitsika[b], Justin J. Nissen[b], Andrew Bowey[c], Thomas J. Joyce[a]

[a]*School of Engineering, Newcastle University, Newcastle Upon Tyne, UK*

[b] *Department of Neurosurgery, Royal Victoria Infirmary, Newcastle upon Tyne, UK*

[c]*Department of Spinal Surgery, Royal Victoria Infirmary, Newcastle upon Tyne, UK*

Abstract

Ex vivo analysis of artificial discs is essential to better understand their ability to replace degenerated intervertebral discs. The Mobi-C differs from some other contemporary disc designs in that it has a mobile polyethylene insert that is sandwiched between superior and inferior cobalt chromium endplates. While some studies claim the Mobi-C to have restored normal cervical spinal biomechanics, others have noted high levels of migration. Our objective was to contribute to this debate by, for the first time, analysing an explanted Mobi-C cervical disc which was removed due to worsening myelopathy at the nano and macro scales. Intraoperatively, the insert was found to have excessively migrated and it compressed the spinal cord. Roughness was measured as 0.016 ± 0.006 µm (Sa) and 0.055 ± 0.020 µm (Sa) for the superior and inferior plates, and 1.210 ± 0.154 µm (Sa) and 0.446 ± 0.083 µm (Sa) for the superior and inferior surfaces of the insert. Compared to unworn surfaces, the roughness increased for the superior and inferior plates and decreased for both surfaces of the insert. However, the only statistically significant change occurred on the articulating surface of the inferior plate ($p=0.04$). At the nanoscale, valleys dominated the articulating surfaces. The superior plate had a burnished appearance whereas the inferior plate appeared matt. Impingement was observed on the endplates. The insert was severely damaged, burnished and had scratches. Additionally, subsurface whitening and internal cracking were observed on the insert.

1. Introduction

The cervical spine consists of 7 vertebrae which are the smallest, yet the most mobile vertebrae of the movable spinal column [1]. Each vertebra is separated by intervertebral discs from one another [1]. Although all intervertebral discs are susceptible to degeneration, the neck is commonly affected [2].

Anterior cervical discectomy and fusion (ACDF) has been the gold-standard treatment for degenerative cervical discs. During this procedure, the disc is removed and a metallic cage is inserted along with bone graft in order to achieve fusion [3]. Nevertheless, ACDF restricts the movement of the vertebrae and can result in progressive degeneration at the adjacent levels [4]. Total disc replacement (TDR) for the cervical spine is considered to be a promising alternative treatment for degenerative disc disease [5]. With TDR, following discectomy (the process of removal of the intervertebral disc), an artificial disc is inserted [5]. As opposed to ACDF, the aim of an artificial disc is to allow pain-free motion [4]. The ball-in-socket geometry is the most common configuration utilised for artificial cervical discs [6]. The most common material combination used is metal-on-polymer (MoP) [7]. Cervical discs that use metal-on-metal (MoM) [7, 8] and self-mating, all-polymer [9] articulations are also available.

TDR is a relatively new treatment compared to total hip and knee replacements, therefore, there are only a few studies that have investigated the biotribological performance of cervical discs [10-12]. Some short-term results, mainly clinical [13-16], of TDR are documented in the literature. However, the efficacy of the artificial discs in replacing natural cervical intervertebral discs remains unknown. The Bryan cervical disc (Medtronic), Prodisc-C (Centinel Spine), Mobi-C (Zimmer Biomet) and M6-C (Orthofix Medical) are examples of cervical discs that utilize MoP articulation. Compared to the Bryan and Prodisc-C discs, the Mobi-C is recently introduced with different design characteristics such that it has a mobile polyethylene insert that is sandwiched between metallic endplates. The positioning of the Mobi-C cervical disc in the prepared, vacant joint space (after discectomy) is done by joint decompression [17]. Once the proper implant size is selected, the superior and inferior endplates are compressed to the vertebrae using distractors (tools that are used to seat the implant between the joint space) [18]. The teeth located at the backsides of the endplates are pressed in the vertebrae with caspar distractors [18]. The titanium and hydroxyapatite coating at the back surfaces of the endplates and the teeth allow fixation of the Mobi-C discs [18]. For explanted MoP cervical discs, failures associated with endplate impingement, polymeric wear debris and innate inflammation have been

reported, while burnishing was a common surface modification noted for the polymeric components [19].

Anderson et al. [13] investigated explanted Bryan cervical discs, after 4 to 11 months in vivo, from 11 patients. The Bryan disc had a bearing articulation formed by titanium plates and polyurethane core [7]. No inflammatory response was recorded in terms of the host response to the device and no wear was recorded from the articulation [10, 13]. Only a colour change was detected for the polymeric component, which appeared more yellow compared to its initial appearance [13]. In a prospective retrieval study conducted by Lebl et al. [14], early clinical failures of thirty Prodisc-C cervical discs from 29 patients after a mean implantation time of 1.0 ± 0.2 years were investigated. The Prodisc-C disc consisted of superior and inferior cobalt chromium (CoCr) endplates (pure titanium coated) and a semi-constrained ultrahigh molecular weight polyethylene (UHMWPE) insert [14]. The surface damage modes observed were burnishing, third body wear and metal endplate-endplate impingement with no backside wear [14]. In terms of clinical results for the Mobi-C cervical disc, from the meta-analysis conducted by Ning et al. [15], encouraging results were recorded. Mobi-C was found to lower pain, resulted in fewer subsequent surgical interventions and a greater range of motion for the operated segment compared to ACDF [15]. The most remarkable finding was, with Mobi-C, the normal spinal biomechanics remained unchanged which avoided the degeneration of the adjacent levels [15]. This finding was not recorded in the aforementioned studies for the MoP designs (for the Bryan and Prodisc-C cervical discs) [13, 14]. Mobi-C discs from 16 patients and M6-C discs from 56 patients, both MoP implants, were compared in terms of the range of motion by Pham et al. [20]. A range of motion of 14.2° ± 5.1° for Mobi-C discs compared to a range of 7.3° ± 4.6° for M6-C discs was recorded, which showed favourable results for the Mobi-C disc, 3 months postoperatively [20]. Alvin and Mroz [16] found that one-level Mobi-C was not inferior nor superior to one-level ACDF. Superior results were obtained for two-level Mobi-C compared to two-level ACDF [16].

Implant and/or insert migration has been reported as an issue mainly for non-constrained cervical discs such as the Mobi-C. Virk et al. [21] investigated 1347 complications reported for Mobi-C, Prodisc-C (fixation to the vertebrae with central keels on both of the titanium plasma coated endplates), Bryan (no direct fixation, fixation is achieved through press-fitting or milling of the titanium porous coated shells), Prestige (fixation to the vertebrae with two toothed keels on the backsides of both of the endplates and titanium plasma spray), M6-C (fixation to the vertebrae with keels on the titanium plasma coated endplates), PCM cervical disc (fixation to the vertebrae with titanium and calcium phosphate coated endplates) and Secure-C (fixation to the vertebrae with multiple serrated keels on the titanium plasma coated endplates). The most common complication recorded was migration, accounting for 25% of the complications (338/1347) and 105 of them were from the Mobi-C discs, which was 30% of the Mobi-C discs analysed. It was noted that migration was the second most common failure mode recorded for the Mobi-C discs following "insertion of device problem" (a complication such as breaking or disassembly of the component(s) during insertion to the cervical spine) [21]. In a study conducted by Choi et al. [22], three groups of goats with three different types of cervical discs namely, Bryan, Prodisc-C and Mobi-C, were analysed. The Bryan discs showed no evidence of migration, only one disc of the Prodisc-C group showed anterior migration after 3 months, and all Mobi-C discs migrated and disintegrated within four weeks. Based on the results of this study [22], one-piece or semi-constrained two-piece cervical discs could be more resistant to migration compared to the unconstrained multi-component discs.

To the best of our knowledge, this is the first study to investigate the biotribological performance of a retrieved Mobi-C disc. The components were analysed both at the nano and macro scales in order to study the explanted Mobi-C cervical disc's in vivo performance.

2. Materials and Methods

2.1 The Mobi-C cervical disc

The articulation of the Mobi-C cervical artificial disc consists of a ball-in-socket. Mobi-C cervical discs have three components: CoCr inferior and superior discs, and a non-constrained, mobile UHMWPE insert. The components are shown in figure 1. The insert sits between the inferior and superior discs. The backsides of the CoCr discs are titanium and hydroxyapatite coated [18]. The superior metallic plate has a recessed spherical contact surface, and the inferior metallic plate has a flat contact surface. Thus, the dome-shaped UHMWPE insert makes a spherical contact with the superior plate with its curved surface and a flat contact with the inferior plate with its flat surface. Both CoCr end plates have two rows of teeth (figure 2b) on their back surfaces (bony interface) opposite to their articulating surfaces. The teeth are designed to improve the initial and long-term fixation of the implant [18]. On the inferior plate, there are two lateral stoppers, shown with arrows in figure 2a, that limit the movement of the UHMWPE insert. The superior plate articulates with the insert and the insert slides across the inferior plate [23].

Figure 1 The Mobi-C cervical disc [23]

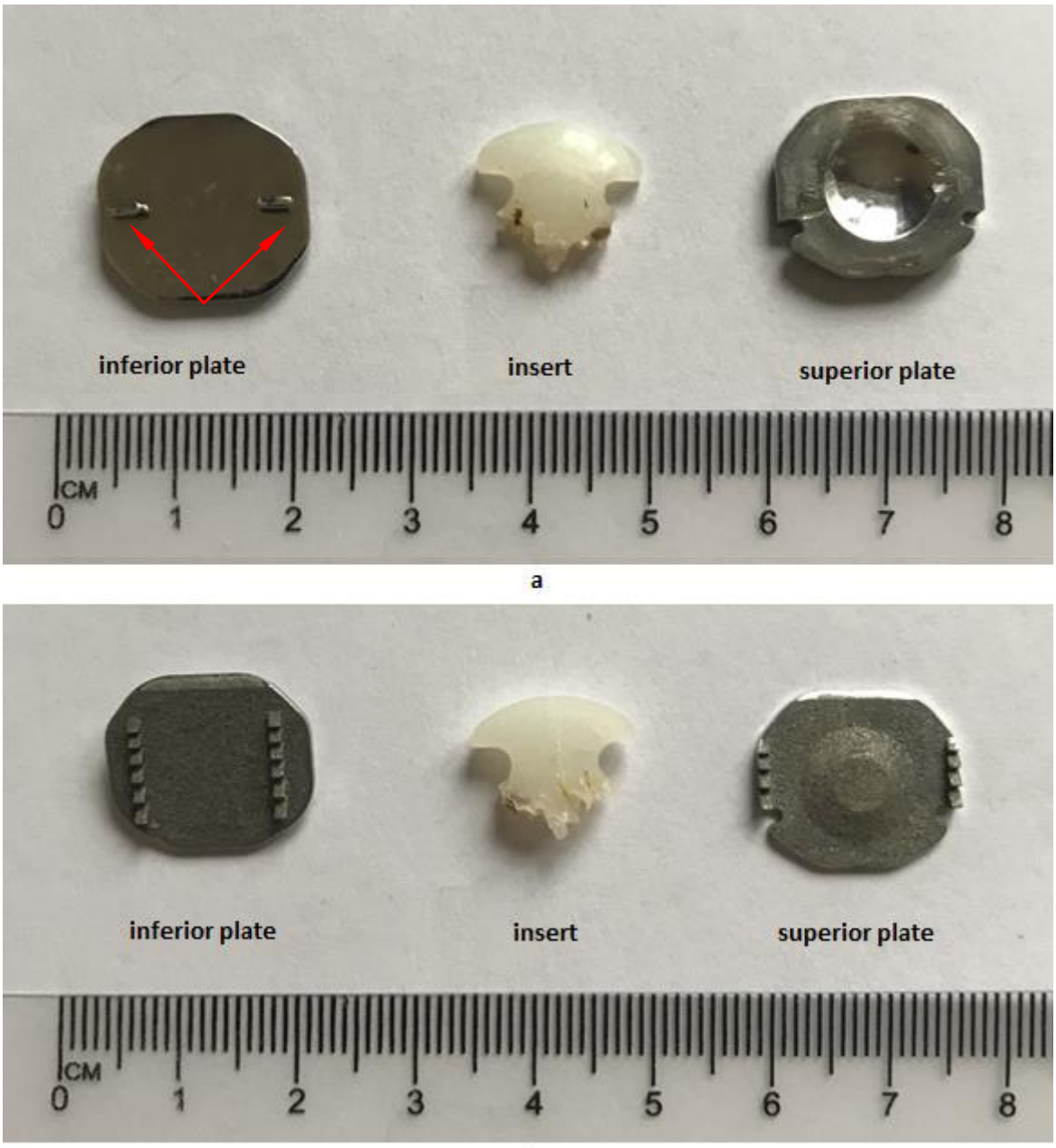

Figure 2 a) The articulating and b) backsides of the inferior (caudal) and superior (cranial) CoCr end plates and UHMWPE insert of the explanted Mobi-C cervical disc. The arrows show the lateral stops on the inferior plate.

The Mobi-C disc was approved by the US Food and Drug Administration (FDA) in 2013 [23] following an earlier introduction outside the United States in November 2004 [15]. It is one of the most widely used MoP cervical discs, and the first and only device approved by the FDA for both single and two-level cervical disc arthroplasty [16] from C3 to C7. The most common complications recorded for artificial discs, including the Mobi-C, were heterotopic ossification (the abnormal bone growth that results in failure of the discs by restricting the range of motion of the replaced vertebrae [24]).

2.2 Explant Analysis

Explant analysis was guided by ISO 12891-2:2020 [25] to conduct a non-destructive macroscopic and microscopic evaluation of the surfaces of the components. The visual and the surface topography analyses conducted by following this guideline gave insights about the wear mechanisms that took place on the surfaces of the insert and the endplates in vivo. The dimensional measurements were taken with a non-contact vision measuring system (Mitutoyo QuickScope), at 25x magnification (50x lens and 0.5x zoom). The surface topographies of the explants were analysed with a Zygo NewView 5000 non-contacting profilometer (which has a sensitivity of 0.001 µm, Ra [26]). Surface topography was assessed with roughness (Sa) and skewness (Ssk) parameters. Surface roughness gives insights about how much the heights of the surface asperities deviate from their ideal form [27]. The tendency of having predominant peaks or valleys can be assessed with the skewness of a surface profile. Before in vivo service, the surfaces of the implants tend to have positive skewness, i.e., they contain more peaks than valleys. When the surfaces interact with other surfaces, they tend to have negative skewness, which means they contain more valleys than peaks [28]. Together, Sa and Ssk can provide information about surface modifications and wear that may occur for surfaces in contact. Twenty measurements were taken from the articulating surfaces. The contact surfaces between the insert and the superior plate and the inferior plate were analysed separately. Since a big portion of the insert was damaged during removal, to strengthen the visual analysis performed, a Hood score analysis was conducted to assess the surface degradation of both surfaces of the UHMWPE insert. Hood analysis is commonly used for polyethylene components, and the assessment is done by analysing seven surface degradation modes (deformation, pitting, embedded debris, scratching, burnishing, abrasion and delamination) [29]. The assessment is further discussed in section 3.3.

2.3 Clinical Details

The 38 year old female patient underwent a C6/7 arthroplasty with the insertion of a Mobi-C Cervical disc prosthesis for myelopathy at a different institute 6 years ago [30]. She presented to our institute

with a three-year history of worsening myelopathy. She underwent extensive investigations to identify the cause for the clinical deterioration. Dynamic (flexion-extension) X-rays of the patient are shown in figure 3.

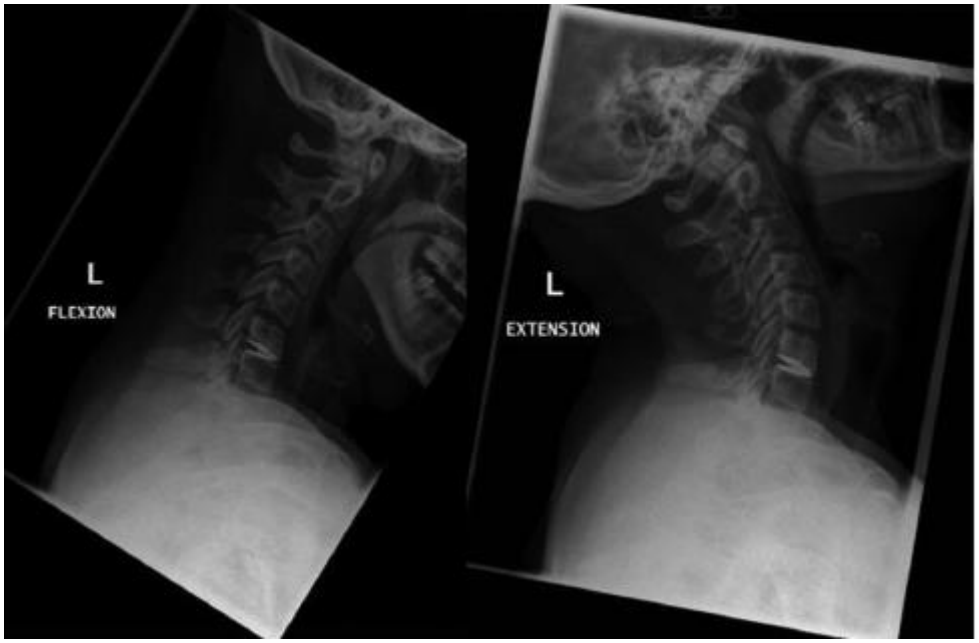

Figure 3 The pre-operative dynamic X-ray images [30].

A lumbar puncture (collecting samples from the cerebrospinal fluid) was done and the results were normal. A Magnetic Resonance Imaging (MRI) showed extensive artefact at the site of the implant making difficult to interpret. A CT myelogram was then performed due to the ongoing clinical deterioration and this showed evidence of cord compression at the site of disc replacement (figure 4) which necessitated removal of the implant. Intraoperative findings consisted of posterior prolapse of the insert of the implant (figure 5) which was compressing the spinal cord. The insert was severely adhered to the dura (the outer membrane of the spinal cord) making it extremely challenging to remove it and the anterior aspect of the insert was severely damaged while attempting to remove it by pulling it out with a rongeur. Eventually, a C6/7 vertebrectomy was done in order to facilitate the removal of the implant (Figure 6). The failure of the implant, in other words the reason for removal, was reported as a late symptomatic complication in the absence of trauma [30].

Figure 4 The CT myelogram showing the ⇒ compressed spinal cord in sagittal (left) and axial views (right) [30].

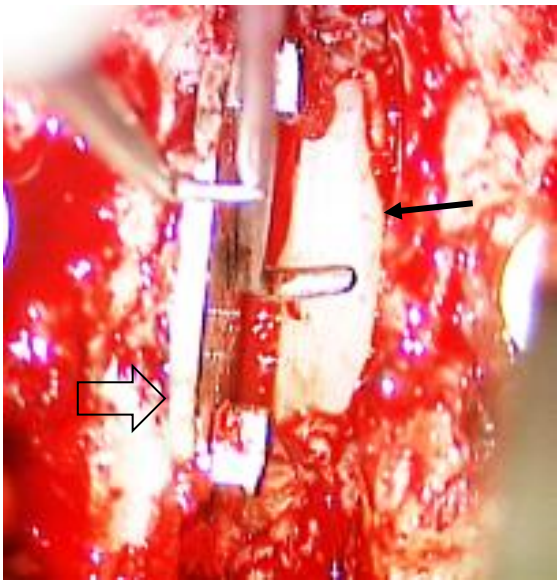

Figure 5 The excessively prolapsed UHMWPE insert (→ shows the insert, ⇒ shows the inferior plate)

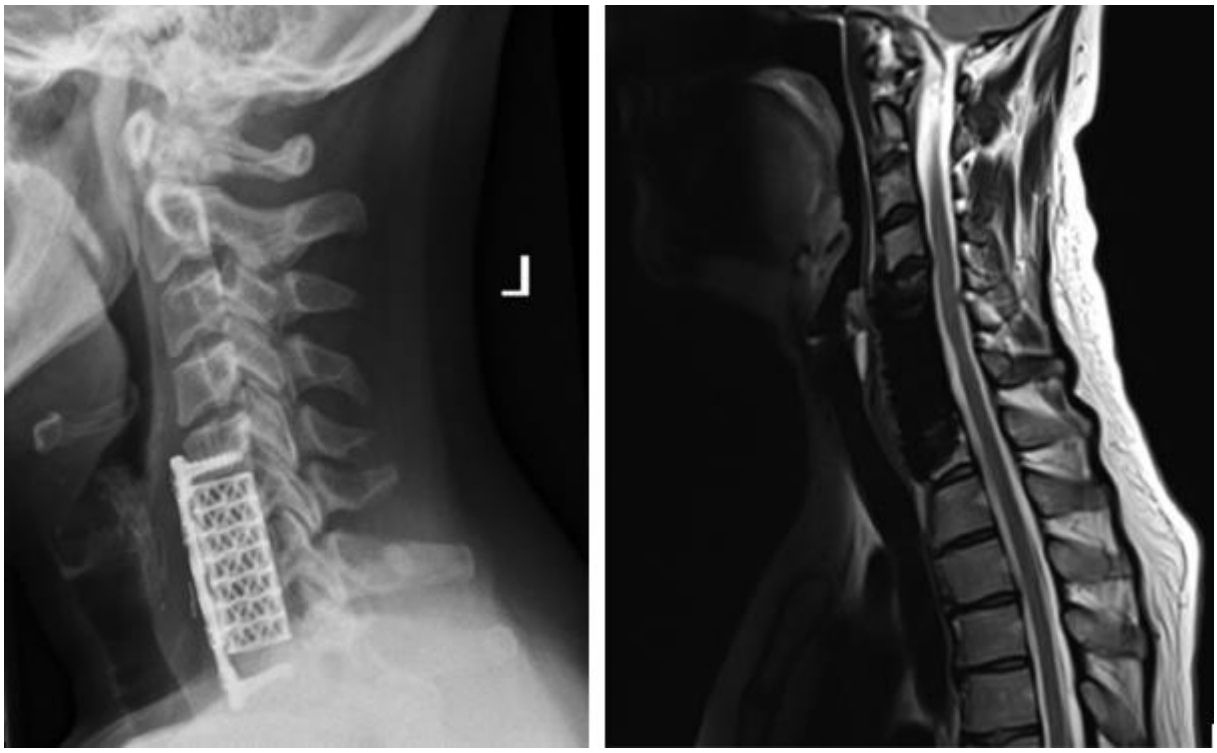

Figure 6 The post-operative X-Ray and MRI scans at 5 months follow-up.

3. Results

3.1 Surface profile analysis

The measured surface roughness data of the articulating surfaces of the Mobi-C disc are provided in table 1.

Table 1 Surface roughness values of the articulating surfaces of the explanted Mobi-C artificial disc.

	CoCr superior (curved) plate	CoCr inferior (flat) plate	UHMWPE curved surface	UHMWPE flat surface
Sa (µm)	0.016 ± 0.006	0.055 ± 0.020	1.210 ± 0.154	0.446 ± 0.083
Ssk	-0.610 ± 0.210	-0.439 ± 0.431	-0.342 ± 0.409	-0.144 ± 0.292

There were no data available for the surface roughness of an unused Mobi-C disc. Therefore, surface roughness values provided in the literature for UHMWPE and CoCr for curved and flat surfaces were used. For the unused curved and flat surfaces of the insert, values of 1.29 ± 0.086 µm [31] and 0.512 ± 0.146 µm [32] were taken. For the superior and inferior plates, values of 0.010 ± 0.003 µm [33] and 0.013 ± 0.004 µm [34] were taken. These roughness values are congruent with ASTM F732-17 [35]

which states that the roughness of a metal prosthesis should be R_a<50 nm. The comparison with the measured values from the explant gave an estimation of how the surface profile changed in vivo (figure 7).

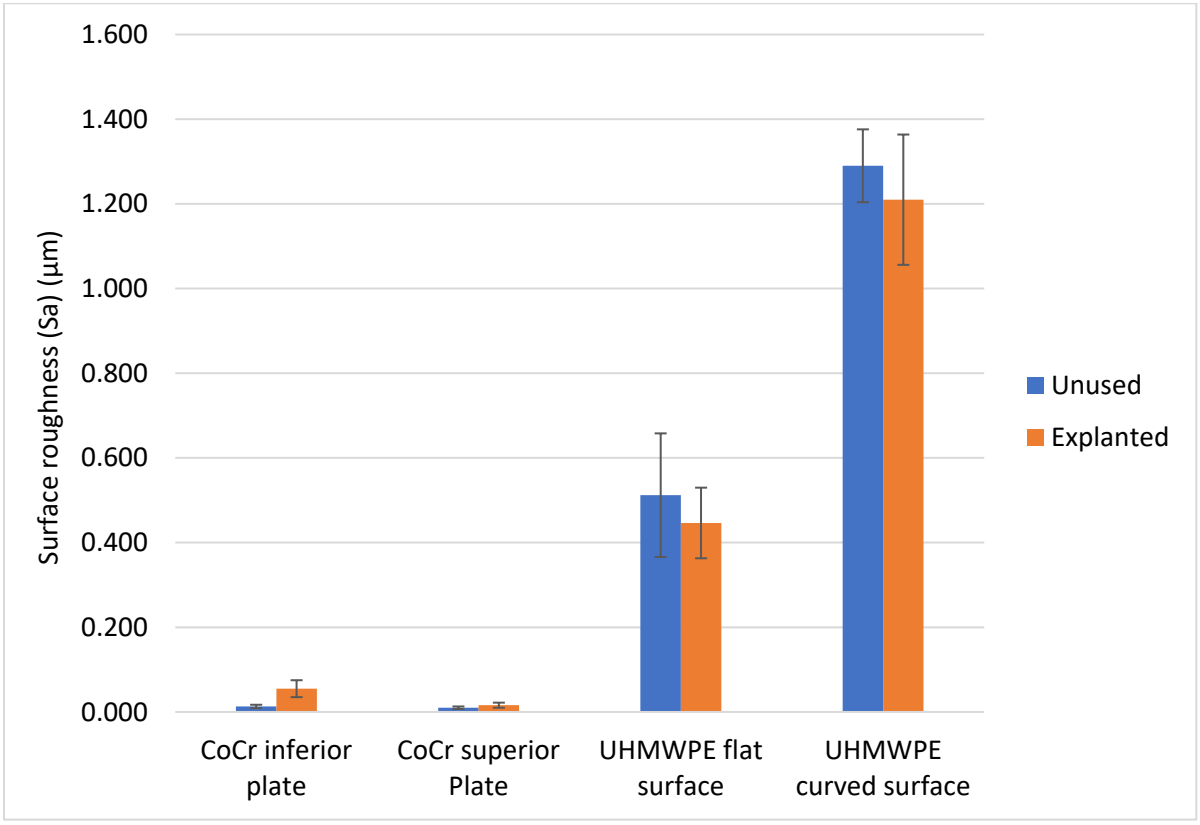

Figure 7 Surface roughness of the articulating surfaces of the unused surfaces and the explanted Mobi-C artificial disc.

The statistical analysis (z-test) for a 95% confidence level of the initial and final values of the surface roughness returned p-values of 0.04, 0.37, 0.70 and 0.65 for the inferior plate, superior plate, flat surface of the insert and curved surface of the insert, respectively. The difference was only significant for the inferior plate. Sample Zygo images for the articulating surfaces are given in figures 8 and 9 for the UHMWPE insert and CoCr plates, respectively.

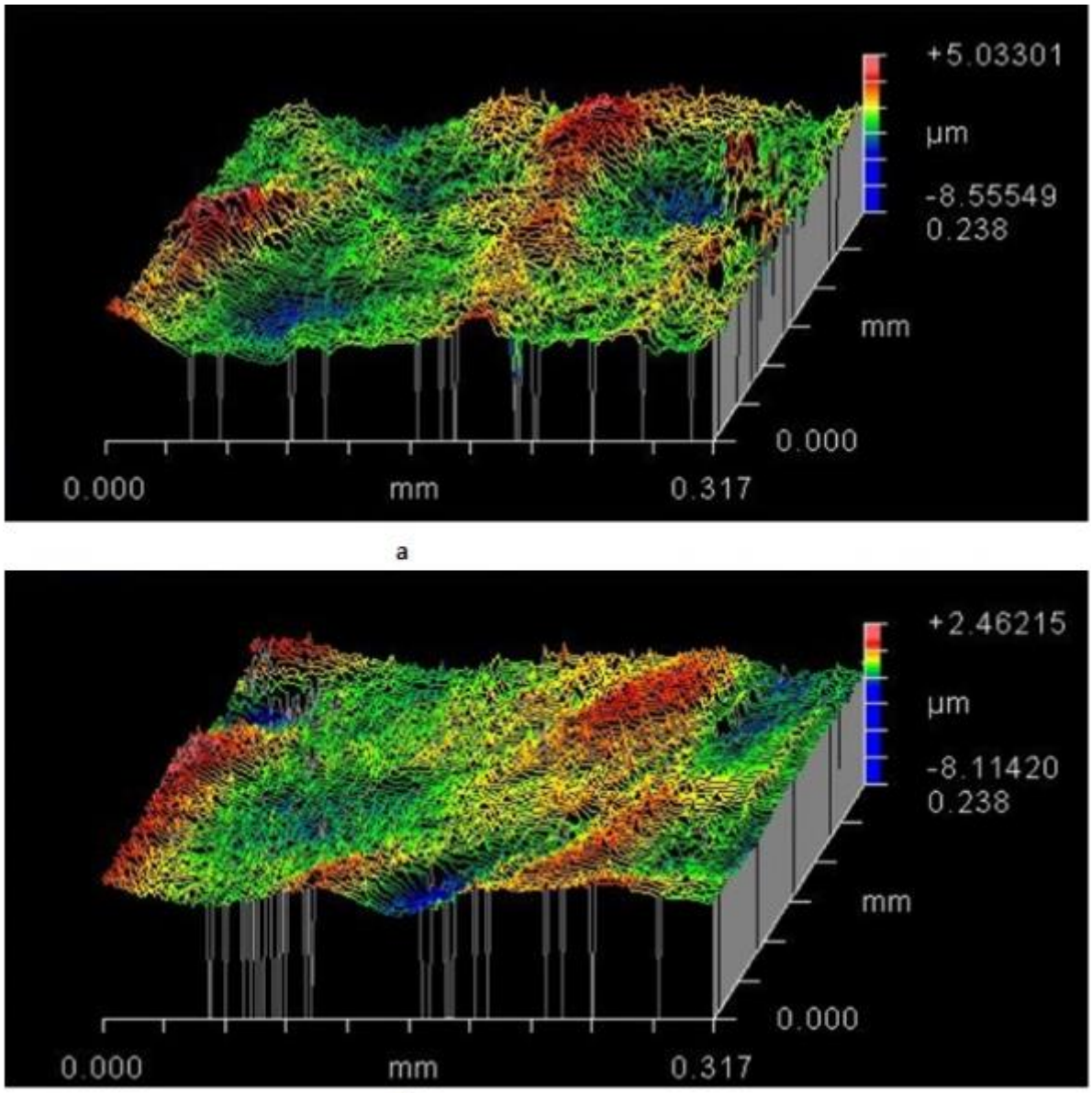

Figure 8 Sample Zygo images of the UHMWPE insert of the Mobi-C artificial disc. a) Curved surface (Sa=0.983 µm, Ssk=-0.463) and b) flat surface (Sa=0.421 µm, Ssk=-0.111)

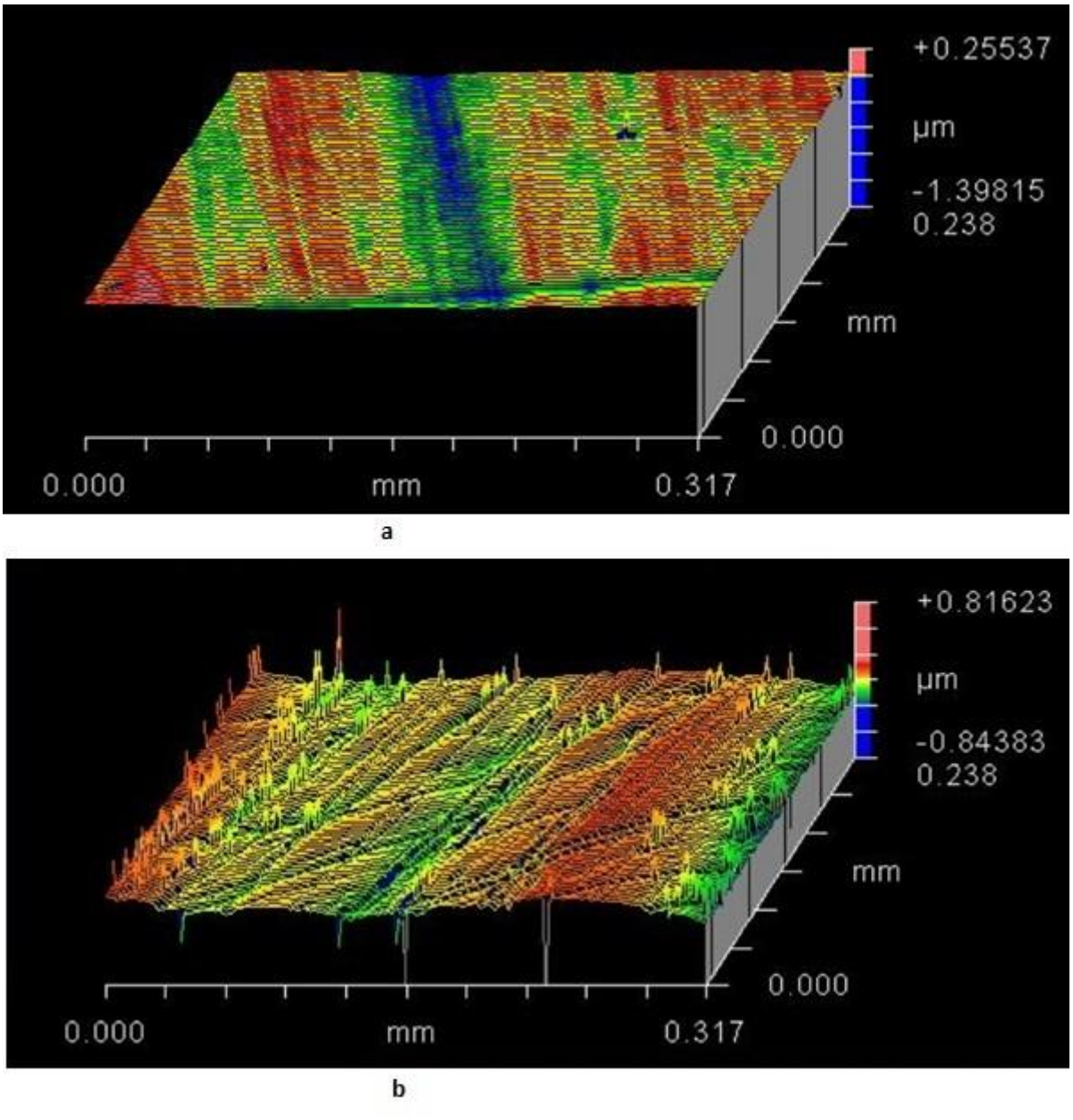

Figure 9 Sample Zygo images of the CoCr plates of the Mobi-C artificial disc. a) Superior plate (Sa=0.011 µm, Ssk=-0.334) and b) inferior plate (Sa=0.050 µm, Ssk=-0.201)

3.2 Visual analysis

The Mobi-C artificial disc was 15 mm in the anterior-posterior direction and 17 mm in the lateral directions. Surface damage modes were examined for the components.

3.2.1 The inferior plate

The flat contact surface formed by the inferior plate and the flat surface of the insert is shown in figure 10.

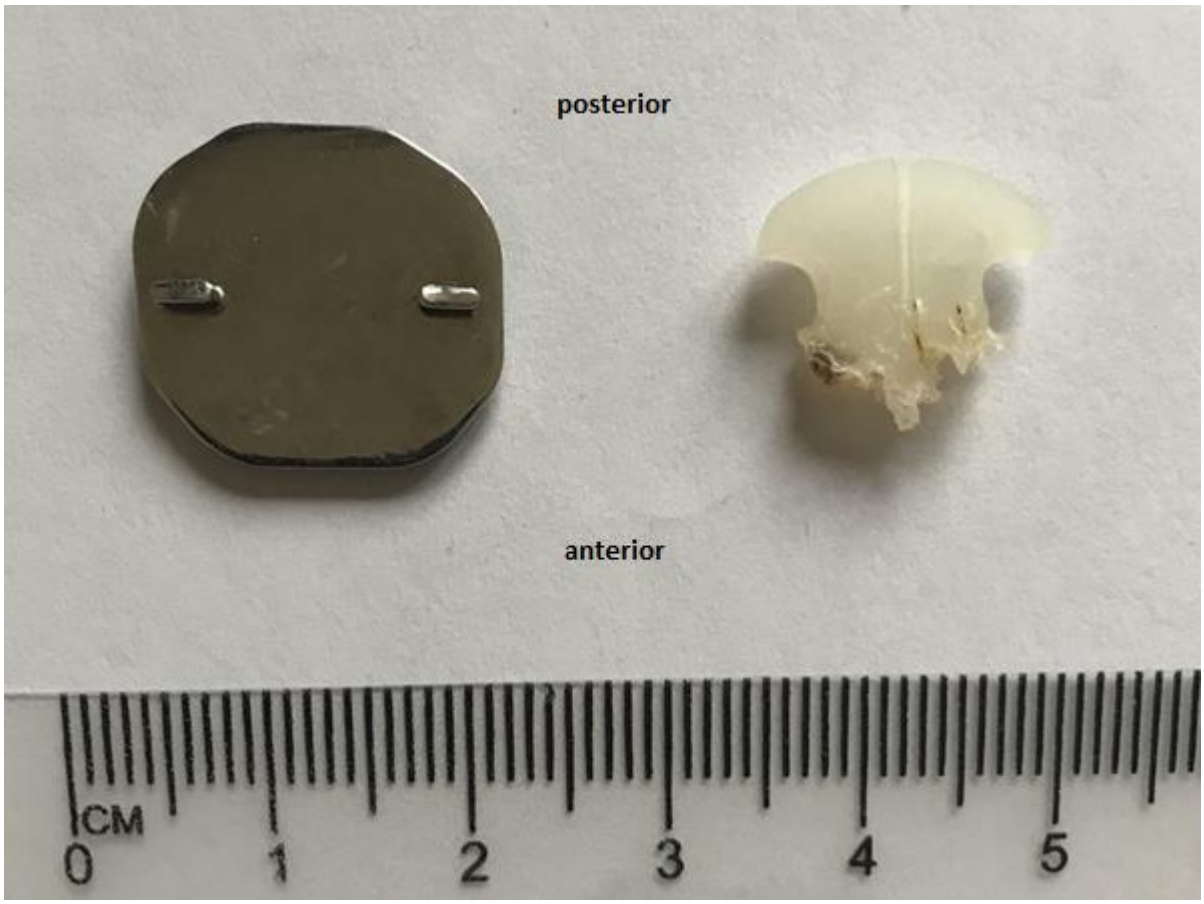

Figure 10 The inferior CoCr plate and the flat surface of the UHMWPE insert, respectively.

The inferior plate lost its polished appearance. Mild scratches were present on the plate. Some traces of pitting were observed near the lateral stops (closer to the anterior edge) and along the area where the UHMWPE insert sat. The top surfaces of the lateral stops were damaged (both 1 mm in length and 0. 1 mm deep). The motion path of the UHMWPE insert was imprinted on the plate (figure 12). There was a scratch (length:8 mm) along the anterior edge of the plate, which appeared darker than the rest of the surface. The surface damages observed are shown in figure 11a. The backside surface and the teeth appeared undamaged. There was only one region that appeared matt compared to the rest of the back surface (figure 11b).

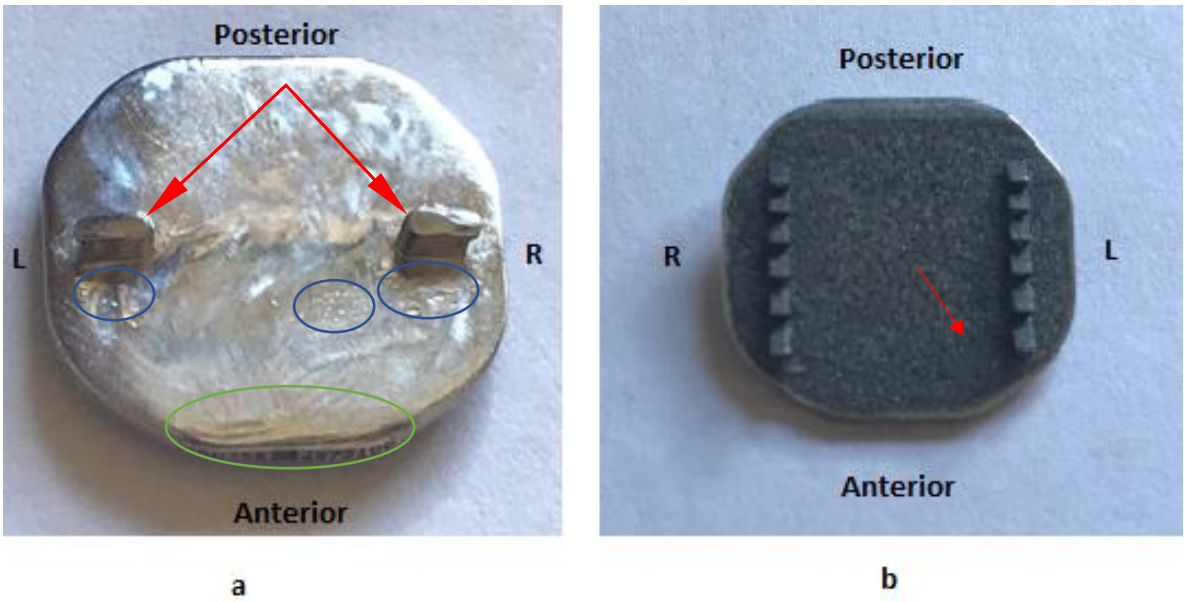

Figure 11 The inferior CoCr plate: a) the articulating surface. The red arrows show the damage on the lateral stops, the blue circles show the pitted regions and the green circle shows the scratch observed at the anterior edge of the endplate, b) The backside. The arrow shows the matt region on the coating.

Figure 12 The articulating surface of the inferior CoCr endplate.

3.2.2 The superior plate

The spherical articulation formed by the superior plate and the curved surface of the insert is shown in figure 13.

Figure 13 The superior CoCr plate and the curved surface of the UHMWPE insert, respectively.

On the superior plate, there were two deep scratches outside and/or at the edges of the articulating curved surface, one on the left lateral side (length: 2 mm, depth: 0.98 mm) and one on the right lateral side (length: 4 mm, depth: 0.91 mm) (figure 14a). These scratches likely occurred due to the formation of a contact between the superior plate and lateral stops of the inferior plate. This observation could be associated with the damage observed on the top surfaces of the lateral stops (figure 11a). There was also one relatively longer (length: 7 mm depth: 0.01 mm) scratch on the anterior side of the superior plate. This region also matched with the damage observed on the anterior edge of the inferior plate (figure 11a). In other words, the anterior edges of the endplates came into contact when the insert slid in the posterior direction.

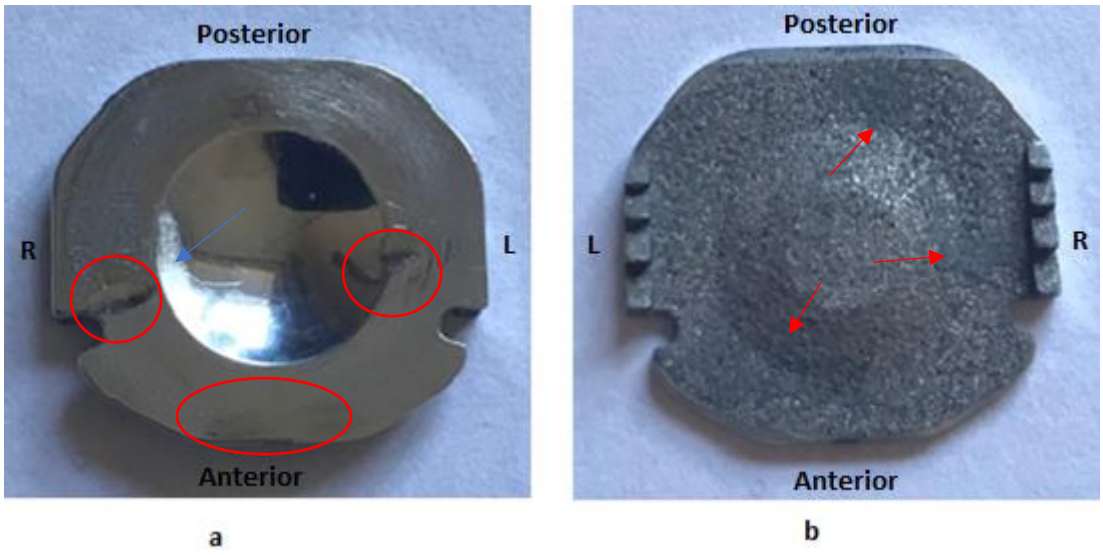

Figure 14 The superior CoCr plate: a) the articulating surface. The red circles show the scratches observed on the left (L), right (R) and at the anterior edge. The blue arrow shows the matt region observed at the curved articulating surface. b) The backside. The arrows show the matt regions on the coating.

The surface that articulated with the insert had a polished appearance. There were mild scratches present all along the articulating surface and there was one region that appeared matt compared to the rest of the surface. The coating of the backside of the superior plate appeared undamaged, however, there were three regions that appeared matt compared to the rest of the surface (figure 14b).

3.2.3. The UHMWPE insert

The UHMWPE insert was highly damaged. A substantial portion from its posterior aspect was damaged during the removal of the implant. As mentioned above, the adherence to the dura made the removal of the insert very difficult.

The curved surface, which was in contact with the superior endplate, was plastically deformed, appeared burnished and was scratched (figure 15a). There were two regions showing subsurface whitening (figure 16a). Internal cracks were observed at its right lateral side (figure 16b). The flat surface, which was in contact with the inferior plate, was also burnished and scratches were present on its surface (figure 15b). No subsurface whitening was observed on the flat surface.

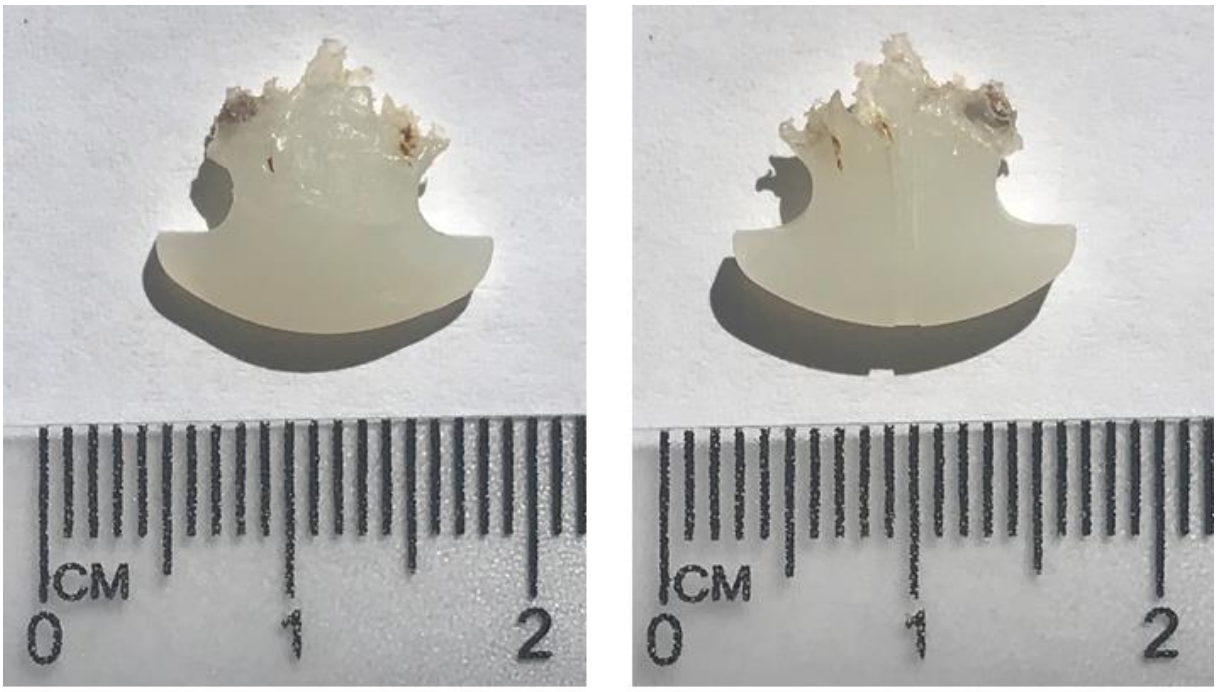

a b

Figure 15 The curved (a) and flat surface (b) of the UHMWPE insert of the Mobi-C artificial disc respectively.

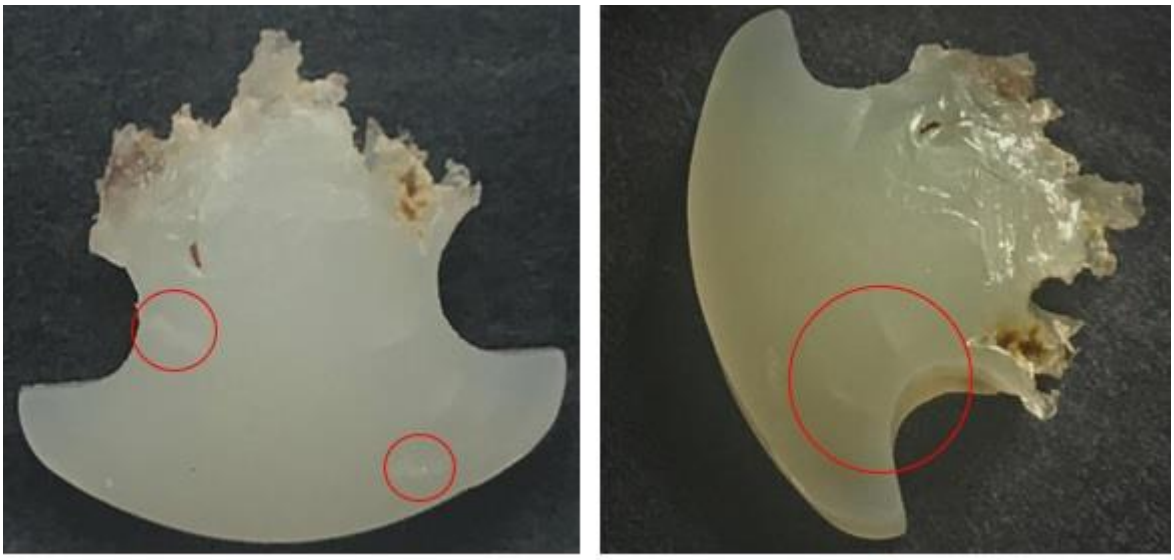

a b

Figure 16 The curved surface of the UHMWPE insert of the Mobi-C artificial disc. a) The circles show the subsurface whitening, b) the circle shows the internal cracking at the lateral side.

3.3 Hood score analysis

Both the top and bottom surfaces of the insert were divided in 4 sections (figure 17) and a Hood analysis was performed. Based on the occurrence of the 7 surface damage modes, 0 (none) - 3 (severe)

scores were assigned to the sections, the minimum score being 0 and the maximum score being 21 per section. The section scores then added up to have a total score for the top and bottom surfaces.

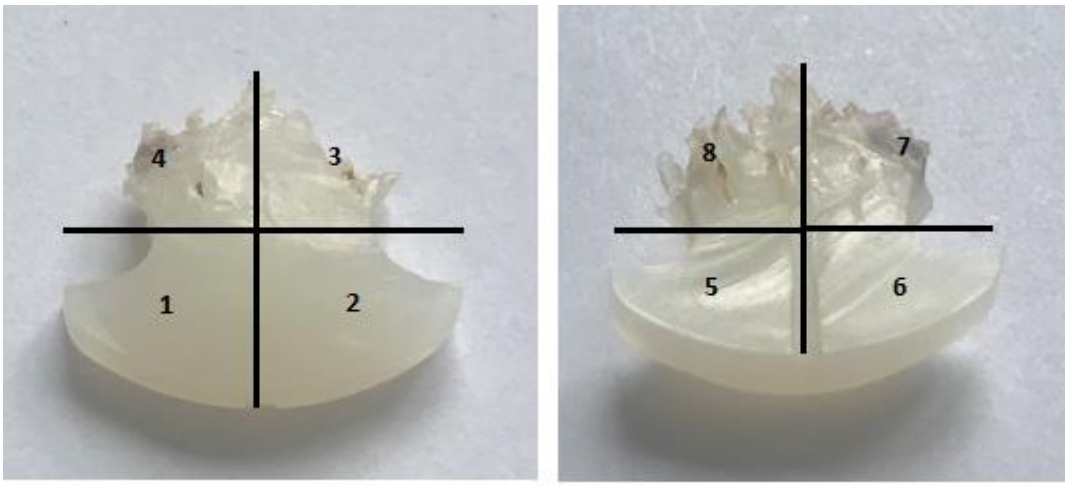

Figure 17 Surface sectioning of the UHMWPE insert used to perform the Hood score analysis.

Based on the analysis, a Hood score of 36 and 35 were calculated for the curved and flat surfaces of the UHMWPE insert respectively. The most common surface degradation modes observed were surface deformation, burnishing and abrasion. Note that the damaged/missing portion, which occurred during removal, from the posterior side was considered as a surface deformation.

4. Discussion

For the first time, a Mobi-C disc, which was explanted due to gradually worsening myelopathy, was analysed at the nano and macro scales with the guidance of ISO 12891-2:2020 [25]. Most noteworthy, the articulating surface of the inferior plate lost its polished appearance. The dull appearance of the inferior endplate could be the result of an increase in its roughness during in vivo service. Polished surfaces tend to have lower roughness compared to surfaces that have dull appearances [36] – as this was also observed for the polished superior plate and matt inferior plate of the explanted Mobi-C disc (see table 1). Howie et al. [36] investigated 24 explanted MoM McKee-Farrar artificial hips (made out of CoCr, and the average time in situ was 16 years) and reported that the explants which had dull appearances had an average surface roughness of 0.056 ± 0.015 (µm ± SD) which showed scratching and wear tracks. For polished (shiny) surfaces, an average roughness of 0.042 ± 0.020 (µm ± SD) was

reported [36]. The reported roughness and the visual observations made by Howie et al. [36] for the dull surfaces of the explanted hips closely matched with the measured average roughness of the inferior endplate (0.056 ± 0.015 (µm ± SD)). Therefore, its matt appearance could be linked to the increase in its surface roughness. The articulating surface of the superior endplate maintained its polished appearance but had mild scratches. The insert was burnished, which is a common observation recorded for explanted polymeric cervical inserts [10, 14, 19], and was severely damaged. The damage mainly occurred during removal. The insert escaped the lateral stops which were supposed to limit its motion in vivo. It adhered to the spinal cord dura which made it very difficult to remove, hence the damage took place. The excessive migration of the insert, shown in figure 5, indicated that the insert was not operating in the intended position (operating between the endplates). This could be the reason of the visual observations made on the articulating surfaces of the endplates, the matt regions and scratches on both of the endplates, the imprinted wear path and pitting on the inferior endplate. The articulating surfaces of the superior and inferior endplates had an average surface roughness of 0.016 µm (Sa) and 0.055 µm (Sa), respectively. The average surface roughness of the curved and flat surfaces of the insert was 1.210 µm (Sa) and 0.446 µm (Sa), respectively. Compared with the suggested initial manufacturing roughness for metal implants (as stated by the ASTM- F732 [35]), the surface roughness was found to increase both for superior and inferior endplates. The roughness of the endplates was also higher when compared to unused curved and flat CoCr surfaces. Although the change was only significant for the inferior plate, the increase in surface roughness of the plates may be important. As shown by Saikko et al. [37], rougher CoCr surfaces tend to remove more material from their UHMWPE counterfaces, which in turn, could result in wear-related issues such as osteolysis. The surface roughness of the insert's curved and flat surfaces was found to decrease compared to unworn curved and flat UHMWPE surfaces. Again, these changes in roughness were not found to be statistically significant, nevertheless, the surfaces had negative skewness. The reduction in roughness and visual observations also suggested material removal. No damage was observed on the

hydroxyapatite coatings of the endplates, only some matt regions were observed which could be a result of an effective osteointegration.

The most common surface damage modes observed for the explant were surface deformation, burnishing and abrasion. These were similar to what has been recorded for other types of MoP cervical discs [10, 14, 19]. Abrasive and adhesive wear mechanisms were dominant with the Mobi-C explant. In addition, traces of subsurface whitening and cracking, and endplate-to-endplate impingement were observed on the surfaces of the explant. These could indicate that other wear mechanisms, i.e., oxidative and fatigue wear, also took place in vivo, in addition to adhesive and abrasive wear.

Scratches were observed on the articulating surfaces of the endplates, i.e., on the lateral stops, outside or at the edge of the articulating surface of the superior plate, and at the anterior edges of both of the endplates. These scratches likely occurred when impingement took place. They also indicated contact between the endplates. The main reason for impingement for the explant was the excessive migration of the insert that resulted in imbalanced loads at the contact regions. Consequently, this metal-to-metal contact could result in metallic debris release.

This study has some limitations. We were unable to quantify the wear generated from the explant. This could not be done for two reasons: first, no unused Mobi-C artificial disc was available for gravimetric/volumetric wear assessment and in addition to that, no information was available in the literature either. However, the nano and macroscale analyses conducted gave insights about the wear mechanisms and the severity of surface deformation modes that took place on the surfaces of the explant in vivo. Another limitation is that the analysis was performed only on a single implant. However, it has been shown that even with a single-sample retrieval analysis, useful information can be obtained [11, 38, 39].

5. Conclusion

With this case study, it was shown that migration can result in clinical complications along with implant failure, especially for non-constrained multi-component disc designs. The insert of the explant analysed in this study prolapsed significantly and compressed the spinal cord causing myelopathy. Consequently it needed to be removed. The roughness of the articulating surfaces of the superior and inferior endplates increased and the roughness of both surfaces of the UHMWPE insert decreased. Only the change in the roughness of the inferior plate was found to be significant. Both the metallic and polymeric surfaces had negative skewness. Unlike the superior plate, the inferior plate had a dull appearance, and the insert's wear path was imprinted on it. Impingement was observed on the surfaces of the endplates. Both surfaces of the insert were burnished and severely damaged.

Source of funding

This research did not receive any specific grant from funding agencies in the public, commercial, or not-for-profit sectors.

Conflicts of Interest: None

Funding: None

Ethical Approval: Not required

6. References

[1] D. A. Neumann, *Kinesiology of the Musculoskeletal System Foundations for Physical Rehabilitation*. St. Louis: Mosby, 2002.

[2] M. A. Secretariat, "Artificial discs for lumbar and cervical degenerative disc disease -update: an evidence-based analysis," Ont Health Technol Assess Ser. , 1915-7398, 2006, vol. 6.

[3] J. M. Rhee and K. L. Ju, "Anterior Cervical Discectomy and Fusion," *JBJS Essential Surgical Techniques,* vol. 6, no. 4, p. e37, 2016, doi: 10.2106/JBJS.ST.15.00056.

[4] W. Wu *et al.*, "Wear assessments of a new cervical spinal disk prosthesis: Influence of loading and kinematic patterns during in vitro wear simulation," *Proceedings of the Institution of Mechanical Engineers, Part H: Journal of Engineering in Medicine,* vol. 229, no. 9, pp. 619-628, 2015, doi: 10.1177/0954411915594829.

[5] S. M. Kurtz *et al.*, "Polyethylene wear and rim fracture in total disc arthroplasty," *The Spine Journal,* vol. 7, no. 1, pp. 12-21, 2007, doi: 10.1016/j.spinee.2006.05.012.

[6] N. C. Green, J. Bowen, D. W. Hukins, and D. E. Shepherd, "Assessment of non-contacting optical methods to measure wear and surface roughness in ceramic total disc replacements,"

Proceedings of the Institution of Mechanical Engineers, Part H: Journal of Engineering in Medicine, vol. 229, no. 3, pp. 245-254, 2015, doi: 10.1177/0954411915577119.

[7] J. P. Clewlow, T. Pylios, and D. Shepherd, "Soft layer bearing joints for spine arthroplasty," *Materials & Design,* vol. 29, no. 10, pp. 1981-1985, 2008, doi: 10.1016/j.matdes.2008.04.008.

[8] S. M. Kurtz, L. Ciccarelli, M. L. Harper, R. Siskey, J. Shorez, and F. W. Chan, "Comparison of in vivo and simulator-retrieved metal-on-metal cervical disc replacements," *The International Journal of Spine Surgery,* vol. 6, no. 1, pp. 145-156, 2012, doi: 10.1016/j.ijsp.2012.03.002.

[9] T. M. Grupp *et al.*, "Alternative bearing materials for intervertebral disc arthroplasty," *Biomaterials,* vol. 31, no. 3, pp. 523-531, 2010, doi: 10.1016/j.biomaterials.2009.09.064.

[10] P. A. Anderson, S. M. Kurtz, and J. M. Toth, "Explant Analysis of Total Disc Replacement," *Seminars in Spine Surgery,* vol. 18, no. 2, pp. 109-116, 2006.

[11] G. Kandemir, S. Smith, J. Andrews, A. Bowey, and T. J. Joyce, "Retrieval analysis of an explanted NuNec cervical disc: A case report," *Biotribology,* vol. 24, p. 100150, 2020/12/01/ 2020, doi: https://doi.org/10.1016/j.biotri.2020.100150.

[12] T. M. Grupp *et al.*, "Biotribological evaluation of artificial disc arthroplasty devices: influence of loading and kinematic patterns during in vitro wear simulation," *European Spine Journal,* vol. 18, no. 1, pp. 98-108, 2009/01/01 2009, doi: 10.1007/s00586-008-0840-5.

[13] P. A. Anderson, J. P. Rouleau, J. M. Toth, and K. D. Riew, "A comparison of simulator-tested and -retrieved cervical disc prostheses. Invited submission from the Joint Section Meeting on Disorders of the Spine and Peripheral Nerves, March 2004," *Journal of neurosurgery. Spine,* vol. 1, no. 2, p. 202, 2004, doi: 10.3171/spi.2004.1.2.0202.

[14] D. R. Lebl, F. P. Jr Cammisa, F. P. Girardi, T. Wright, and C. Abjornson, "The mechanical performance of cervical total disc replacements in vivo: prospective retrieval analysis of prodisc-C devices," *Spine,* vol. 37, no. 26, pp. 2151-2160, 2012.

[15] G. Z. Ning, S. L. Kan, R. S. Zhu, and S. Q. Feng, "Comparison of Mobi-C Cervical Disc Arthroplasty Versus Fusion for the Treatment of Symptomatic Cervical Degenerative Disc Disease," *World Neurosurgery,* vol. 114, pp. e224-e239, 2018, doi: 10.1016/j.wneu.2018.02.169.

[16] M. D. Alvin and T. E. Mroz, "The Mobi-C cervical disc for one-level and two-level cervical disc replacement: a review of the literature," *Medical devices (Auckland, N.Z.),* vol. 7, pp. 397-403, 2014, doi: 10.2147/MDER.S54497.

[17] D. Leven, J. Meaike, K. Radcliff, and S. Qureshi, "Cervical disc replacement surgery: indications, technique, and technical pearls," *Current Reviews in Musculoskeletal Medicine,* vol. 10, no. 2, pp. 160-169, 2017, doi: 10.1007/s12178-017-9398-3.

[18] *Mobi-C Cervical Disc Surgical Technique Guide*. USA: Zimmer Biomet.

[19] S. Veruva, M. Steinbeck, J. Toth, D. Alexander, and S. Kurtz, "Which Design and Biomaterial Factors Affect Clinical Wear Performance of Total Disc Replacements? A Systematic Review," *Clinical Orthopaedics and Related Research®,* vol. 472, no. 12, pp. 3759-3769, 2014, doi: 10.1007/s11999-014-3751-2.

[20] M. Pham, K. Phan, I. Teng, and R. J. Mobbs, "Comparative Study Between M6-C and Mobi-C Cervical Artificial Disc Replacement: Biomechanical Outcomes and Comparison with Normative Data," *Orthopaedic Surgery,* vol. 10, no. 2, pp. 84-88, 2018, doi: 10.1111/os.12376.

[21] S. Virk, F. Phillips, S. Khan, and S. Qureshi, "A cross-sectional analysis of 1347 complications for cervical disc replacements from medical device reports maintained by the United States Food and Drug Administration," *The Spine Journal,* 2020/09/20/ 2020, doi: https://doi.org/10.1016/j.spinee.2020.09.005.

[22] H. Choi, J. L. Baisden, and N. Yoganandan, "A Comparative in vivo Study of Semi-constrained and Unconstrained Cervical Artificial Disc Prostheses," *Military Medicine,* vol. 184, no. Supplement_1, pp. 637-643, 2019, doi: 10.1093/milmed/usy395.

[23] *Mobi-C Cervical Artificial Disc Patient Education*. USA: LDR Spine, 2013.

[24] N. Hui, K. Phan, J. Kerferd, M. Lee, and R. J. Mobbs, "Comparison of M6-C and Mobi-C cervical total disc replacement for cervical degenerative disc disease in adults," *Journal of spine surgery (Hong Kong),* vol. 5, no. 4, pp. 393-403, 2019, doi: 10.21037/jss.2019.09.27.
[25] *BS ISO 12891-2:2020 Retrieval and analysis of surgical implants — Part 2: Analysis of retrieved surgical implants*. 2020.
[26] T. J. Joyce, H. Grigg, D. J. Langton, and A. V. F. Nargol, "Quantification of self-polishing in vivo from explanted metal-on-metal total hip replacements," *Tribology International,* vol. 44, no. 5, pp. 513-516, 2011, doi: 10.1016/j.triboint.2010.04.007.
[27] R. Holleyman *et al.*, "Changes in surface topography at the TKA backside articulation following in vivo service: a retrieval analysis," *Knee Surgery, Sports Traumatology, Arthroscopy,* vol. 23, no. 12, pp. 3523-3531, 2015, doi: 10.1007/s00167-014-3197-9.
[28] S. Scholes *et al.*, "Topographical analysis of the femoral components of ex vivo total knee replacements," *Journal of Materials Science: Materials in Medicine,* vol. 24, no. 2, pp. 547-554, 2013, doi: 10.1007/s10856-012-4815-z.
[29] R.W. Hood, T. M. Wright, and A. H. Burstein, "Retrieval analysis of total knee prostheses: A method and its application to 48 condylar prostheses," *Journal of Biomedical Materials Research,* vol. 17, pp. 829-842, 1983.
[30] M. Pitsika and J. Nissen, "Spinal cord compression due to nucleus migration from Mobi-C total disc replacement," *British Journal of Neurosurgery,* pp. 1-4, 2020, doi: 10.1080/02688697.2020.1716942.
[31] S. C. Scholes and A. Unsworth, "Comparison of friction and lubrication of different hip prostheses," *Proceedings of the Institution of Mechanical Engineers, Part H: Journal of Engineering in Medicine,* vol. 214, no. 1, pp. 49-57, 2000, doi: 10.1243/0954411001535237.
[32] K. Vassiliou and A. Unsworth, "Is the wear factor in total joint replacements dependent on the nominal contact stress in ultra-high molecular weight polyethylene contacts?," *Proceedings of the Institution of Mechanical Engineers, Part H: Journal of Engineering in Medicine,* vol. 218, pp. 101-107, 2004. [Online]. Available: http://journals.sagepub.com/doi/pdf/10.1243/095441104322983997.
[33] S. L. Smith, D. Dowson, and A. A. J. Goldsmith, "The lubrication of metal-on-metal total hip joints: A slide down the Stribeck curve," *Proceedings of the Institution of Mechanical Engineers, Part J: Journal of Engineering Tribology,* vol. 215, no. 5, pp. 483-493, 2001, doi: 10.1243/1350650011543718.
[34] G. Kandemir, S. Smith, and T. J. Joyce, "The influence of contact stress on the wear of cross-linked polyethylene," *Proceedings of the Institution of Mechanical Engineers, Part H: Journal of Engineering in Medicine,* vol. 232, no. 10, pp. 1008-1016, 2018, doi: 10.1177/0954411918796047.
[35] "ASTM International. F732-17 Standard Test Method for Wear Testing of Polymeric Materials Used in Total Joint Prostheses," ed, 2017.
[36] D. W. Howie, R. W. McCalden, N. S. Nawana, K. Costi, M. J. Pearcy, and C. Subramanian, "The Long-Term Wear of Retrieved McKee-Farrar Metal-on-Metal Total Hip Prostheses," *The Journal of Arthroplasty,* vol. 20, no. 3, pp. 350-357, 2005/04/01/ 2005, doi: https://doi.org/10.1016/j.arth.2004.09.028.
[37] V. Saikko, O. Calonius, and J. Keränen, "Wear of conventional and cross-linked ultra-high-molecular-weight polyethylene acetabular cups against polished and roughened CoCr femoral heads in a biaxial hip simulator," *Journal of biomedical materials research,* vol. 63, no. 6, pp. 848-853, 2002, doi: 10.1002/jbm.10471.
[38] T. J. Joyce, "Examination of failed ex vivo metal-on-metal metatarsophalangeal prosthesis and comparison with theoretically determined lubrication regimes," *Wear,* vol. 263, no. 7, pp. 1050-1054, 2007, doi: 10.1016/j.wear.2006.11.045.
[39] G. Kandemir, S. Smith, I. Schmidt, and T. J. Joyce, "Explant analysis of a Maestro™ wrist prosthesis and calculation of its lubrication regime," *Journal of the mechanical behavior of biomedical materials,* vol. 110, p. 103933, 2020, doi: 10.1016/j.jmbbm.2020.103933.

467